Characterization of Shear-Thickening Fluid-Filled Foam Systems for Use in Energy Absorption Devices

by

Jose G. Ramirez

SUBMITTED TO THE DEPARTMENT OF MECHANICAL ENGINEERING
IN PARTIAL FULFILLMENT FOR THE DEGREE OF

BACHELOR OF SCIENCE
AT THE
MASSACHUSETTS INSTITUTE OF TECHNOLOGY
[June 2004]
MAY 2004

Signature of Author: ____________________
Department of Mechanical Engineering
May 7, 2004

Certified by: ____________________
Gareth McKinley
Professor of Mechanical Engineering
Thesis Supervisor

Accepted by: ____________________
Ernest G. Cravalho
Professor of Mechanical Engineering
Chairman, Undergraduate Thesis Committee

Characterization of Shear-Thickening Fluid-Filled Foam Systems for Use in Energy Absorption Devices

by

Jose G. Ramirez

Submitted to the Department of Mechanical Engineering
on May 7, 2004 in Partial Fulfillment of the
Requirement for the Degree of Bachelor of Science in
Mechanical Engineering

ABSTRACT

The absorption of energy during impacts is ubiquitous in society. From our car seats to body armor, the ability to divert or dissipate unwanted energy is an aspect that has many engineering challenges. One approach to this issue is the use of fluid-filled elastomeric foams. In the present thesis, the fluid within these foams is a non-Newtonian shear-thickening fluid composed of 300 nm silica particles suspended in a solvent, ethylene glycol, at high concentrations, 45-55 %. The field of energy absorption using elastomeric foams has been extensively researched in industry. In addition, the effects and mechanism driving shear-thickening fluids (STF's) has also been well studied in industries involving particle suspensions, such as paints and medical applications. This research intends to combine the analysis of these two systems in an effort to characterize advanced energy absorption mechanism. It was found that the primary factors dominating fluid filled foams containing this STF are the volume fractions and compressional strain rate. In addition, the energy absorption capability of these foams has been compared to that of 'dry' foams and Newtonian-fluid filled foams, and has demonstrated an increase in energy absorption capabilities.

Thesis Supervisor: Gareth H. McKinley

Title: Professor of Mechanical Engineering

Acknowledgements

I would like to express my deepest gratitude to my mentor, Giorgia Bettin, who patiently guided me throughout the process of this research. I have grown as a person and as an engineer as a result of this guidance. Her vast knowledge of this field as well as her unique troubleshooting methods have given me a new perspective on approaching the obstacles of life.

Table of Contents

List of Figures

1: Introduction and Motivation

1.1 *Background: Energy Shunting Materials*

The ability to shunt energy during impacts is critical to many applications where delicate materials need to be protected. These applications range the spectrum of packaging materials for transportation to bodily garments for protecting against environmentally induced impacts. One application, specific to this research, is the use of energy shunting devices in splints or other biomedical devices. The energy absorbing materials used in these applications include elastomeric foams. These foams use the bending and elastic buckling of the foam's cell walls, as well as the viscous dissipative effects incurred when expelling fluids in the foam cells, for energy absorption.

1.2 *Motivation and Problem*

The motivation for this project is to develop an understanding of the energy shunting mechanism found in shear-thickening-fluid (STF) impregnated elastomeric foams. The reason for this selection is motivated by previous works in this area, as well as the beneficial characteristics provided by these two materials. US Patents 5599290 and 5545128 have developed a, "Bone fracture prevention garment and method". In these two works, carried out by the same authors, the patent outlines a design used to resolve the issue of the harmful effects of impacts on the bones of elderly individuals. This design is described as being composed of the following: "the component includes a dilatant material that is relatively stiff near the time of impact and relatively fluid at other times. In a preferred embodiment, the invention provides a hip pad, possessing a thickness small enough to be compatible with wearer acceptability, that conforms to the shape of the body during everyday activities such as walking, sitting, and sleeping, and is thus comfortable to the wearer" (Hayes 1997). However, in an attempt to expand this design onto other applications, it is necessary to characterize the specific elements involved in a 'successful' energy shunting system.

As such, the research intends to characterize the parameters that are important in energy shunting systems involving shear-thickening-fluid filled elastomeric foams. Using the extensive research involving shear-thickening fluids, as well the research done in the energy absorption capabilities of foam, a combined methodology is developed to characterize this system. From the perspective of the fluids, the specific aspects that have been studied include the property of increasing viscosity with increased fluid shear rate, as well the two 'Newtonian plateaus' that are characteristic of the fluid. Thus, the specific mechanisms involved with these two properties have been well defined, and these parameters are included in this research and analysis. In addition, the specific mechanisms needed to analyze foam systems are well developed and are used in this research.

2: Shear Thickening: Introduction and Literature Review

"Shear Thickening is defined in the British Standard Rheological Nomenclature as the increase of viscosity [of a fluid] with increase in shear rate," (Barnes 1989). In addition, according to Barnes, shear-thickening has been considered a problem in many industrial applications including the mixing, coating, milling, or spraying of these fluids. However, it is intended, in this research, to use the results found to control shear-thickening in a manner that would be beneficial to our energy shunting system.

2.1 Shear Thickening Fluids: Introduction

Shear-thickening fluids are concentrated colloidal suspensions composed of nonaggregating solid particles suspended in fluids. These suspensions have the property of increasing the fluid viscosity with increasing shear rate. In addition, this increased viscosity is seen as being both 'field activated', due to the dependency on shearing rate, as well as reversible. In particular, the property that makes it 'field' activated is the critical shear rate ($\dot{\gamma}_c$), which increases the viscosity of the suspension, as shown in figure 1.

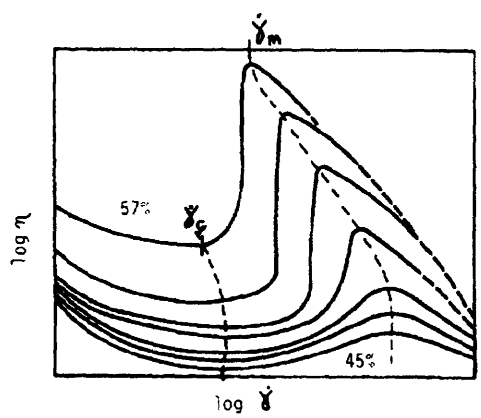

Figure 1 Representation of Shear-Thickening Behavior using a viscosity versus shear rate plot, in a logarithmic representation (Barnes 1989)

In addition, the suspension behaves as a 'Newtonian' fluid during a large spectrum of shear rates, except for the transition shear rate period that causes the fluid's specific critical shear rate transition. These types of fluids have been characterized as behaving as quasi-Newtonian fluids with a low viscosity (η_L) before the critical shear rate transition, and, again, with a quasi-Newtonian behavior but with a higher viscosity (η_H) after the transition. (Laun et al.).

In order to model the rheological behavior of these fluids, it has been proposed to use a power law analysis with the relationship between the viscosity and shear rate represented by

$$\eta = \kappa\dot{\gamma}^{n-1} \tag{1. 1}$$

where κ is the fluid's consistency and n is the power law exponent specific to the region of high or low viscosity. According to Barnes, the shear-thinning and shear-thickening regions can be accounted for by, "using the sum of two power laws, with one value of n less than unity and one greater" (Barnes 1989).

2.2 Parameters Controlling Shear-Thickening

The shear thickening properties exhibited by concentrated dispersions can be controlled by several different parameters. In particular, research has shown a critical shear-rate dependency on the volume fraction of the particles in the suspension as well as the particle dimension, demonstrated by the following functional relationship,

$$\dot{\gamma} \propto f(\phi, a, \zeta, \ldots) \tag{2. 2}$$

where ϕ is the volume fraction of particles in the suspensions ($\frac{V_{particles}}{V_{solvent}}$), and a is the particle radius. Extensive amounts of research have been done to determine the dependence of shear thickening on these two parameters.

2.2.1 Dependence on Volume Fraction

One parameter that has a large effect on the critical shear rate is the volume fraction. This topic of volume fraction dependence is the initial starting point of many researchers, who have found that the shear rate, as well as the increase in viscosity, is highly dependent on this parameter. At low volume fractions, $\phi < 0.5$, shear thickening is either less dramatic or not significant. This effect can be seen in the work by van der Werff and De Kruiff, who were able to demonstrate the dependence of volume fraction on the shear-thickening, while using different sized spherical particles.

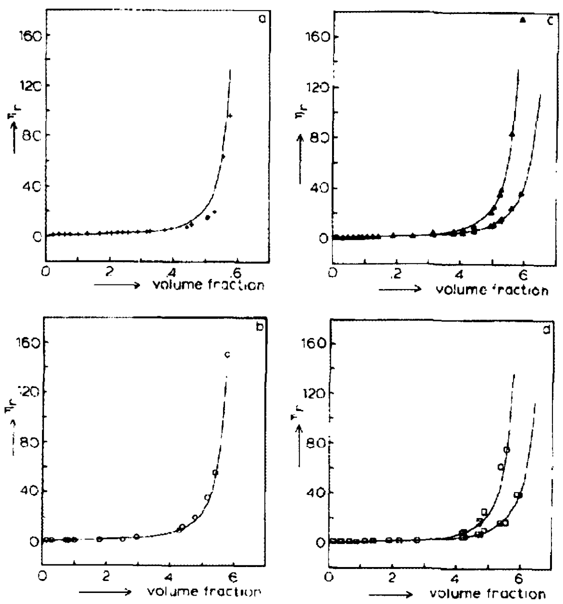

Figure 2 Effect of volume fraction dependence on increase in viscosity in concentrated suspensions. The particle radius used in each of the four plots, are as follows, read in a clockwise fashion starting with the top left plot: 28, 46, 76, and 110 nm radius (van der Werff and De Kruif 1989).

It can be seen, as expected, that the viscosity of the non-Newtonian fluid increases with increasing volume fraction. In addition to affecting the viscosity, the critical shear rate is also dependent on this parameter, as 'thickening' occurs at lower shear-rate values when the suspension has a high volume fraction, and vice versa. The dependence of shear rate on volume fraction was further analyzed and interpreted by Barnes, who analyzed the data of several researchers. His analysis demonstrates that the dependence can be represented by the schematic in figure 3.

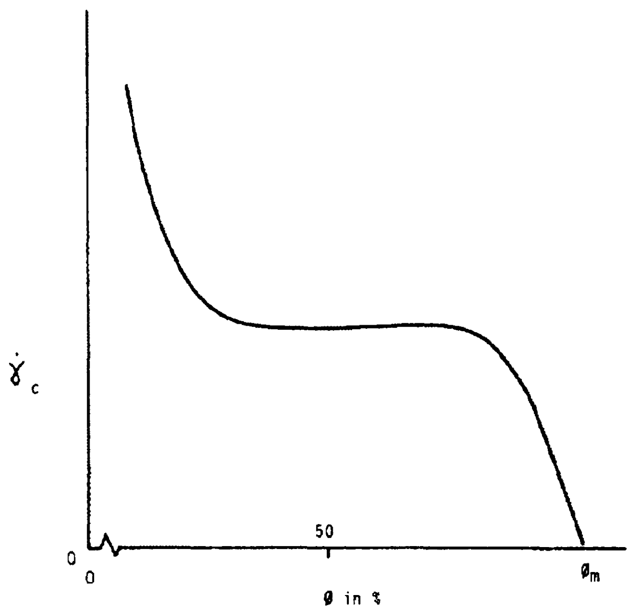

Figure 3 Schematic representation of the dependence of the critical shear rate as a function of the volume fraction (Barnes 1989)

The results of Barnes demonstrate that at volume fractions in the range of 50 %, the shear thickening behavior is expected and predictable. In addition, theoretical analysis of the maximum volume fraction of monodisperse suspensions predicts this value is ϕ_{max} =0.605, where this value corresponds to, "the volume fraction for a cubically stacked hexagonal packing" (Boersma et al.).

2.2.2 Dependence on Particle Size

The size of the particles in the suspensions has a large effect on the value of the critical shear rate. If we consider the particles to be spherical in nature, the radius of these particles can be seen to have an inverse quadratic dependence on the shear rate (Barnes 1989),

$$\dot{\gamma}_c \propto \frac{1}{a^2} \tag{2. 3}$$

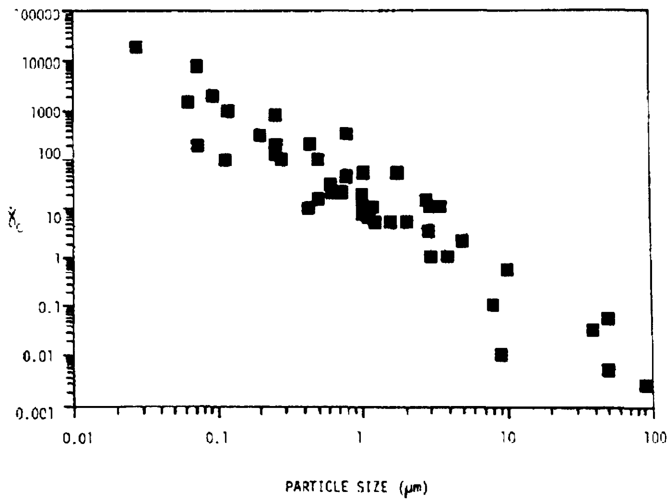

Figure 4 Dependence of critical shear rate ($\dot{\gamma}_c$) on particle size (a) (Barnes 1989)

As will be developed in the next section, the dependence of these two values fits very well with the theoretical interpretation of the interparticle interactions during the shearing of the fluid.

2.3 Theoretical Model of Shear Thickening

2.3.1 Interparticle Analysis

The analysis used to describe the behavior of shear-thickening in concentrated dispersions is found by analyzing the forces that take place between particles. This analysis is based on a force balance between the interparticle forces and the hydrodynamic forces. According to Boersma, "when the shear forces overcome the repulsive interparticle forces, there is a transition to shear thickening". As a result of this analysis, a model has been developed to determine the critical shear rate, which is given by

$$\dot{\gamma}_c = \frac{2\pi\varepsilon_0\varepsilon_r\psi_0^2}{6\pi\eta_0 a}\frac{k}{2}\frac{h}{a} \propto \frac{1}{a^2} \tag{2. 4}$$

where ε_r is the relative dielectric constant of the medium, ε_0 is the permittivity of vacuum ($8.854\times10^{-12}\frac{C}{Vm}$); ψ_0 is the surface potential, which can be approximated by the ζ potential of the particles in the medium; η_0 is the medium viscosity; a is the particle radius; $1/k$ is the Debye double layer thickness; and h is the distance between the particles (Boersma et al.). Thus, the analytical results are representative of the constitutive model, which verifies the inverse square relationship found in Barnes's analysis. In addition, according to Boersma, the ratio $\frac{h}{a}$ is given by the following expressions,

$$\frac{h}{a} = \left(\frac{8\pi}{3\sqrt{3}\phi}\right)^{\frac{1}{3}} - 2 \propto \frac{1}{\phi^6} \qquad (2.\ 5),$$

which correlates equation 2.4 to the volume fraction of the suspension (Boersma et al.). Combining equations 1.1, 2.4, and 2.5, one is able to derive the following relationship between the relative viscosity of the suspension and the volume fraction of the suspensions,

$$\eta \propto \phi^6 \qquad (2.\ 6).$$

This relationship corresponds well with the relationship shown in figure 2, the empirical model.

3: Cellular Solids: Review

3.1 Structure and Properties of Foams

3.1.1 Introduction and Cell Structure

Open-cell flexible foams are important industrial materials with widespread use in household furniture and car seating. The cushioning application of these materials depends critically on how they deform under a compressive load. According to Lakes, “Cellular solids, depending on microstructure, can be very efficient in terms of optimizing strength and stiffness with respect to weight. Foam materials have often been called ‘nature’s equivalent of the I-beam’” (Lee 1997), see figure 4.

Figure 5 Scanning Electron Micrograph (SEM) image of a cut surface of polyurethane foam under 45 % strain (Lee, 1997)

It is well understood that the deformation of open-cell foams shows three main regimes: an initial linear elastic regime, where the strain energy is stored in the reversible bending of the struts; a plateau regime, where small increases in load lead to very large additional strain; and finally a densification regime where struts begin to impinge upon each other. During the final stage, the foam essentially becomes a solid composed of the solid material from which it is made. These three regions can be easily distinguished in stress-strain plots taken during the compression of foams, see figure 5.

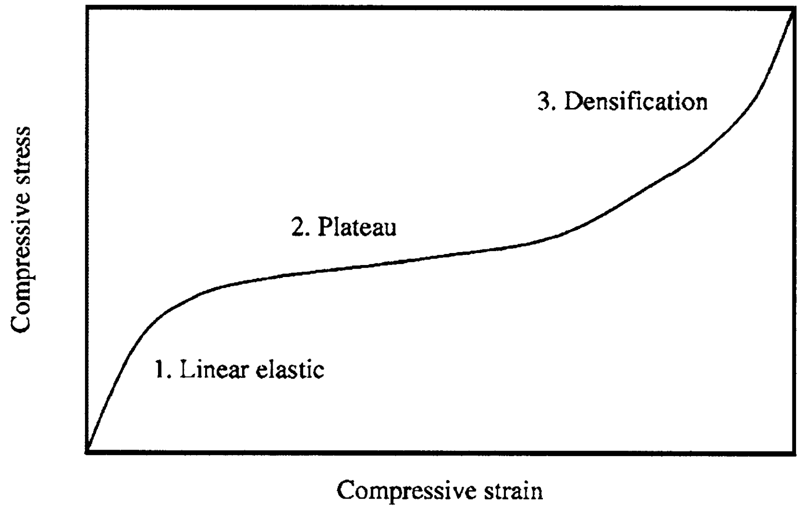

Figure 6 Schematic of a stress-strain curve for an open-cell flexible polyurethane foam, showing three deformations regimes; linear elastic, plateau and densification (Lee, 1997)

3.1.2 Properties of Cellular Solids

The mechanical properties of the cellular solids are dependent upon the properties of the foam's cell structures. The general method of analysis models the cell as, "a cubic array of members of length l and square cross-section of side t" (Lu 1999), figure 7.

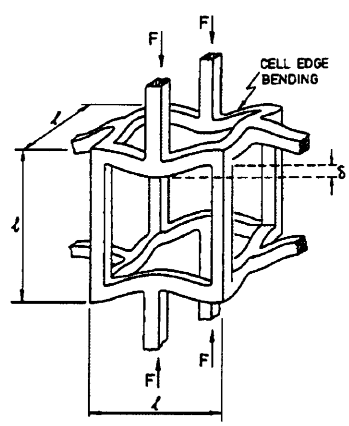

Figure 7 Theoretical model of a foam cell under a load (Lu 1999)

From this model, the defining characteristics relative to cell structures can be found. The principle characteristic describing foams is the relative density ($\frac{\rho *}{\rho_s}$) which is the ratio between the foam's density ($\rho *$) to that of the solid material (ρ_s), (Lu 1999). The relationship between the geometry and physical parameters describing the cell and the relative density is given by the following relationship (Lu 1999)

$$\frac{\rho *}{\rho_s} \propto \left(\frac{t}{l}\right)^2 \qquad (3.\ 1).$$

From this relationship, the porosity of the foam can be found

$$\phi = 1 - \frac{\rho *}{\rho_o} \qquad (3.\ 2).$$

In addition, another important property used in determining the mechanical properties of materials is the elastic modulus. Although foams are inherently anisotropic, a general relationship using the previous analysis and some empirical results is given by

$$E = E_s(1-\phi)^2 \qquad (3.\ 3)$$

where E_s is the elastic modulus of the solid material (Lee 1997).

3.2 Mechanics of Foams

3.2.1 Foams in Compression

Foams are used in energy absorbing applications due to their mechanical behavior that makes them optimal for this. In particular, foams are able to dissipate large quantities of energy due to the elastic, plastic, and buckling modes that occur during compression. As such, the compressive behavior is analyzed by means of stress-strain testing that reveals these energy absorption modes.

As described earlier, foams have three characteristics regimes during compression. In the elastic regime, the behavior is elastic and all of the energy in this region tends to be restored. However, during the plateau region, Euler buckling tends to dominate, since the cell struts in the foam tend to collapse during this area of strain. Since the work done to collapse those struts is the area under the stress-strain curve, it is obvious that this region of the strain is primary mode of energy dissipation, figure 8.

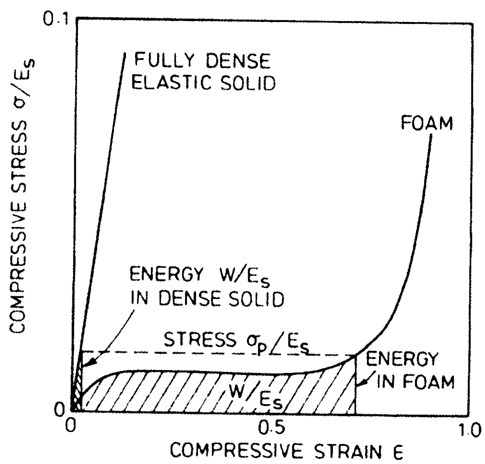

Figure 8 Stress-strain curve for an elastic solid and a foam made from the same solid (Gibson and Ashby, 1997)

During the densification regime, the foam is compressed to point where it behaves as a solid. The strain (ε_D) where the foam behaves as a solid mass is found by to be related to the relative density ($\frac{\rho^*}{\rho_s}$) by the following (Gibson and Ashby, 1997),

$$\varepsilon_D = 1 - 1.4\left(\frac{\rho^*}{\rho_s}\right) \qquad (3.4).$$

3.2.3 Energy absorption in foams

The energy absorbed by the foams can be found by taking the area under the curve of figure 8, or by the following relationship, (Gibson and Ashby, 1997),

$$W = \int_0^{\varepsilon} \sigma(\varepsilon) d\varepsilon \qquad (3.5).$$

Using this equation, energy-absorption diagrams can be constructed that relate the amount of energy that foam can dissipate at specific loads, see figure 9. These foams compare the energy required to compress a load with the stress at the specific strain. In order to compare different types of foams, these plots are normalized by the elastic modulus of the solid material used to form the foams.

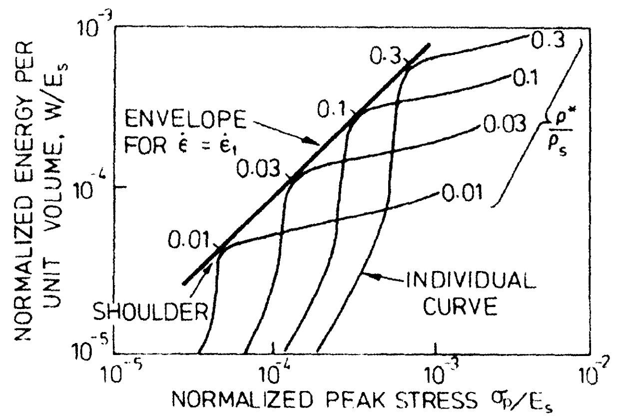

Figure 9 Work versus Stress Plots derived from figure 8 using equation 3.5 (Gibson and Ashby, 1997)

It can be noted, from figure 9, that as the relative density of the foam increases, $(\frac{\rho^*}{\rho_s})$, the overall energy absorption capability also increases at higher stresses. This energy absorption capability plateaus out at a specific stress, representative of the densification region. Using this property, foams can be optimized for specific uses by selecting the foam according to the densification of the foam at a specific stress.

3.2.4 Fluid-filled foams in compression

Besides the energy dissipation that is visible from the mechanical properties of the cell structure, another form of energy dissipation is found in the viscous work done to expel fluid from inside the cells of the foam. This mechanism is generally not considered since most foams are filled with air; however, this mechanism becomes an issue when the fluid viscosity increase. When the viscous effect becomes significant, then the work required to compress a foam filled with this fluid is described by

$$\frac{W}{E_s} = 0.05\left(\frac{\rho^*}{\rho_s}\right)^2\left(1-1.4\frac{\rho^*}{\rho_s}\right)+\frac{C\mu\dot{\varepsilon}}{E_s}\left(\frac{L}{l}\right)^2\left(\frac{1}{1.4\frac{\rho^*}{\rho_s}}\right) \tag{3. 6}$$

where $\dot{\varepsilon}$ is the compressive strain-rate of the foam; μ is the viscosity of the fluid; L is the original length of the sample; and l is the characteristic length of the foam cell, (Gibson and Ashby, 1997). In addition to affecting the work required to compress the foam, the addition of a viscous fluid to the foam also changes the densification strain (ε_D) of the foam. The new densification strain (ε_N) can be found by

$$\varepsilon_N = \varepsilon_D(1-\phi_v) \tag{3. 7}$$

where ϕ_v is the volume fraction of fluid volume in foam to overall foam volume (v/v). As a result, a general relationship relating the foam properties and the fluid inside the foam is given by

$$\varepsilon_N = \left(1-1.4\left(\frac{\rho^*}{\rho_s}\right)\right)(1-\phi_v) \tag{3. 8}$$

4: Theoretical Model for Shear Thickening Fluid-Filled Foams

4.1 Theoretical Model of Shear-Thickening Fluid Filled Foam

It can be seen from equation 3.6 that if the viscosity of the fluid inside of the foam is large, then a large amount of work will be done to compress the foam. In the case of shear-thickening fluid filled foams, there is a large dependence on the energy absorption capabilities related to the fluids viscosity. Since the parameter controlling the viscosity behavior of these fluids is highly dependent upon the shear-rate on the fluid, it is necessary to determine a relationship between the properties of the foam to those of the fluid inside the foam cells. An analysis done by Deshmukh determined an analytical description of the, "shear rate of the fluid inside the capillary," as

$$\dot{\gamma} = \left(\frac{\partial v}{\partial r}\right) \approx \left(\frac{4\phi_v \dot{\varepsilon}(1-\varepsilon)L_0}{l}\right) \qquad \text{(3. 9) (Deshmukh 2003).}$$

Using equations 1.1, 3.4, 3.6, 3.9, one can infer the following relationships between the work done to compress the shear-thickening fluid filled foam completely and other physical parameters by the following relationship

$$W_C \propto \phi_v^{\,2} \dot{\varepsilon}^2 \left(\frac{\rho^*}{\rho_S}\right) \qquad (3.\ 10)$$

As such, it can be seen that the work done to compress the foam is dependent upon the following physical parameters: it is dependent upon the volume fraction (ϕ_v) of the fluid volume inside of the foam; as well as the compressive strain rate ($\dot{\varepsilon}$) applied; and the relative density ($\frac{\rho^*}{\rho_S}$) of the foam.

5: Experimental Methods and Materials

5.1 Procedures for Making Shear-Thickening Fluids

Pure silica (Mol. Wt. 60.09) was used in all of the experiments. The particles were spherical and monodispersed. The particle size was 300 nm, with particle size distribution of 11%. The dispersions were composed of silica (SiO_2) particles suspended in ethylene glycol (ρ= 1.113 g/cm3, μ_o= 0.021 P.s). In order to achieve high volume fractions, ϕ_v>0.50, the particles were initially suspended at low concentrations, ϕ_v=0.20, in the said solvent. During this stage, the particles were sonicated in order to achieve the uniform dispersion that results from the ultrasonic preparation. According to Perez-Rodriguez, "sonication produces not only a delaminating effect [...] but also a breaking of layers in the other directions, while the crystalline character is retained," (Perez-Rodriguez 2002). Sonication was carried out for two hour periods, which was seen to be the time period necessary for the production of completely non-aggregated colloidal suspensions. After sonication, the suspension were centrifuged for a total of six hours (ω=3600 rpm, T = 23°C). This process of centrifugation enabled highly-packed concentrations on the order of $\phi_v \approx 0.60$, which is close to the maximum packing fraction for suspensions. At this, point, the hard packed suspensions were separated from the supernatant. In the final stage, the suspensions were suspended to concentrations of $\phi_v \approx 0.52$ by adding proportional amounts of solvent to partially reduce the total concentration.

5.2 Characterizing Rheological Properties of Suspension

5.2.1 Density Measurement of Silica Particles

The density of the silica particles was determined via a regression analysis. During this analysis, a DMA 35N Density Meter, manufactured by Anton Paar USA, was used to measure the density of variable concentration suspensions, ϕ_v<0.30.

Figure 10 DMA 35N Density Meter by Anton Paar (www.anton-paar.com)

By comparing the increase in mass of the concentrations with the change in density of the overall suspension, found via the density meter, the density of the silica particles was determined, see figure 11.

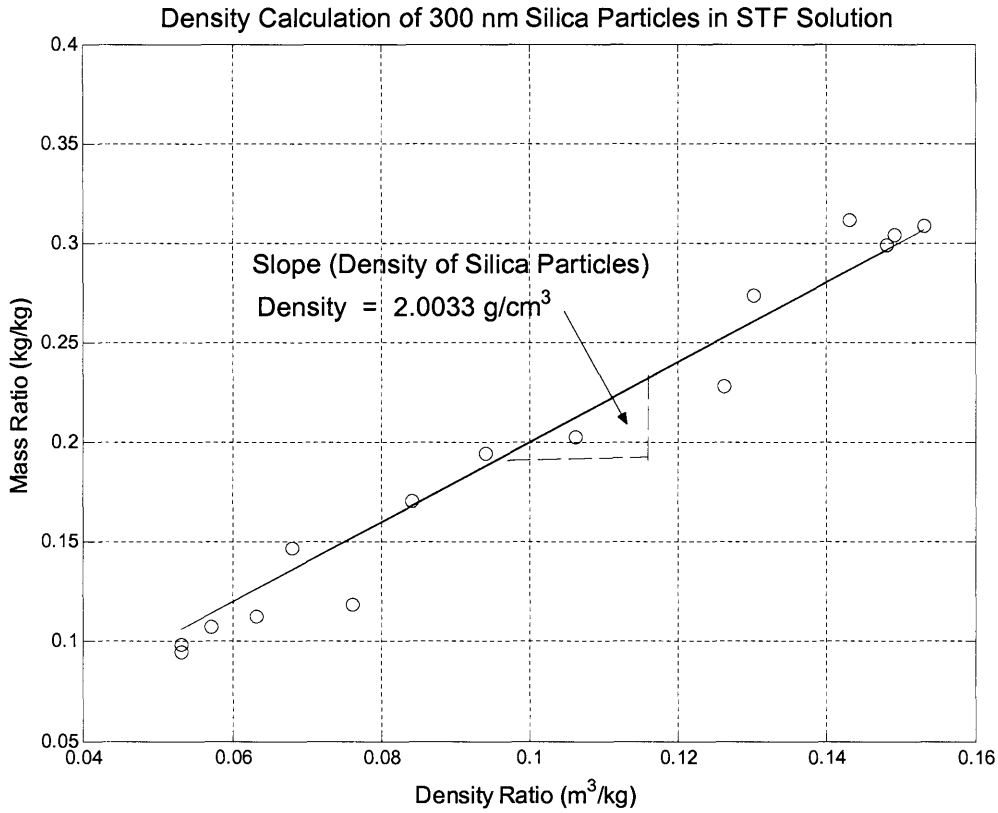

Figure 11 Results of regression analysis for density measurement of silica particles

It was found that the density of the silica particles was 2.003 g/cm^3, a value well within our expected range. According to Maranzano and Wagner (2001), it has been found that amorphous bulk silica has a density of 2.2 g/cm^3. In addition, previous research with silica particles has determined densities on the order of 1.8 g/cm^3.

5.3 Method and Materials

5.3.1 Standard Test Methods for Foams

ASTM Standard D3574-03 is the standard used for testing of urethane foams. Specifically, the name of the standard is, “Standard Test Methods for Flexible Cellular Materials-Slab, Bonded, and Molded Urethane Foams,” (ASTM). Due to the nature of our materials, this standard was used to determine the criteria needed to tests our samples.

The specific test method that was used in this standard was the following, "Test C- Compression Force Deflection Test". It was stated that specimen used during tests should have, "thickness shall be no greater than 75% of the minimum top dimension". As such, the general dimensions of the samples tested in this research had the following dimensions: the diameter and height of the specimen were 28, and 20 mm, respectively.

5.3.2 Testing apparatus for foams

Testing consisted of compression tests carried out on a Texture Analyzer, a low strain-rate compression testing device that is used specifically for semi-solid and foam samples. This device, manufactured by Stable Microsystems Inc., was used due its high resolution at low strain rates, 10^{-3} mm displacement resolution.

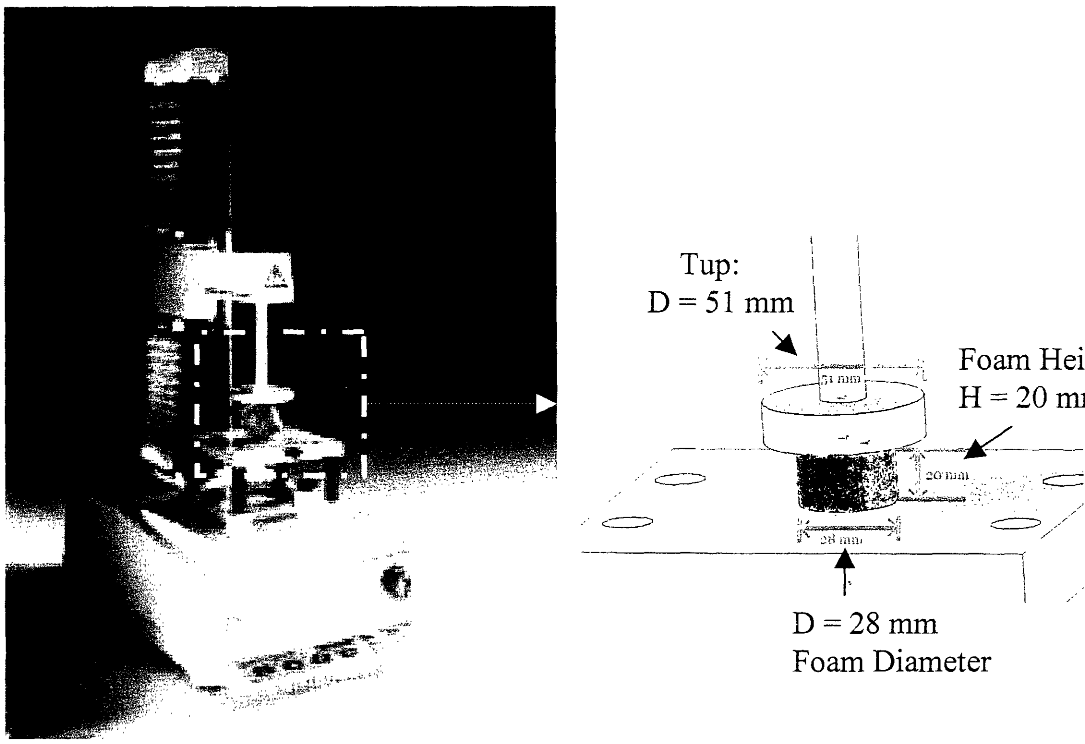

Figure 12 a) TA.XT2 Texture Analyzer, a low strain rate testing equipment for foams and semi-solid materials (<www.stablemicrosystems.com>) b) Schematic of compression specimen in texture analyzer: Dimensions for compression specimens were 28x20 mm, diameter and height, respectively.

Specifically, the testing done during this research consisted of constant strain-rate testing at rates ranging from 0.1 to 10 s^{-1}.

5.3.3 Materials

The polyurethane foam was obtained from Crest Foam Industries, Inc., located in Moonachie, NJ. The foam is reticulated with an open cell structure. The foam was provided in samples of 30x30x8 cm. The material was then cut into cylindrical specimens with a diameter of 28 mm and a length of 20 mm. The method in which these samples were cut involved stamping the foam with a standard 3.175 cm open die, which had an inner diameter of 28 mm.

Table 1: Properties of polyurethane foam (www.crestfoam.com)

Indsutry Foam Characteristic	Category	Density of Foam	Density of PU	Relative Density	Porosity	Cell Length	Young's Modulus of Foam	Young's Modulus of PU
pores per inch	S-Grades	ρ^*	ρ_s	$\frac{\rho^*}{\rho_s}$	ϕ	d	E	E_s
ppi		kg/m^2	kg/m^3	%		μm	Pa	Pa
70	S-70	~0.03	1.05~1.25	2.4~2.9	~0.97	850	~2.16	$69*10^6$
50	S-50	~0.03	1.05~1.25	2.4~2.9	~0.97	500	~2.16	$69*10^6$
30	S-30	~0.03	1.05~1.25	2.4~2.9	~0.97	363	~2.16	$69*10^6$

In addition to testing the foam in its 'dry' state, the foam was also tested under two other conditions: 1) the foam was filled with a Newtonian fluid, glycerol; and 2) the foam was filled with a non-Newtonian fluid, a shear-thickening fluid. The fluids were impregnated into the foams via the slow suction of fluids by uncompressing the samples immersed inside of the specific fluid. The volume fraction of the fluid inside of the foam was determined via weight measurements and the following relationship

$$\phi_v = \frac{\dfrac{m_{total} - m_{foam}}{\rho_{suspension}}}{V_{foam}}$$

Several samples with a spectrum of volume fractions were made. Since the overall distribution within the foams was not tested, the mechanical results are considered an average value.

6: Results

6.1 Rheological Properties of Fluids

The physical properties of the shear thickening fluids were found via rheological testing carried out on an AR2000 rheometer, manufactured by TA Instruments (Bettin).

Table 2: Properties of Shear Thickening Fluids

Critical Shear Rate	Critical Shear Stress	Density of Suspension	Particle Radius	Surface Potential	Viscocity of solvent	Relative Temperature	Volume Fraction
$\dot{\gamma}_c$	τ_c	ρ	a	ζ	μ_o	T	ϕ
1/s	Pa	g/cm^3	μm	mV	Pa.s	Kelvin	% (v/v)
20	20	2.003	150	-50	0.021	293	52

6.2 Results and Discussion: Mechanical Properties of Dry and Impregnated Foams

6.2.1 Dry foams under compression

The characteristics of the foams used in this research were found by means of stress-strain analysis as described in Section 5.3. The specific foam used in this research was the polyurethane foam of cell size d=363 μm. The stress-strain response of the foam, at three different strain rates, $\dot{\varepsilon} = 0.5$, 1.0, and 5.0 s^{-1}, is shown in figure 13.

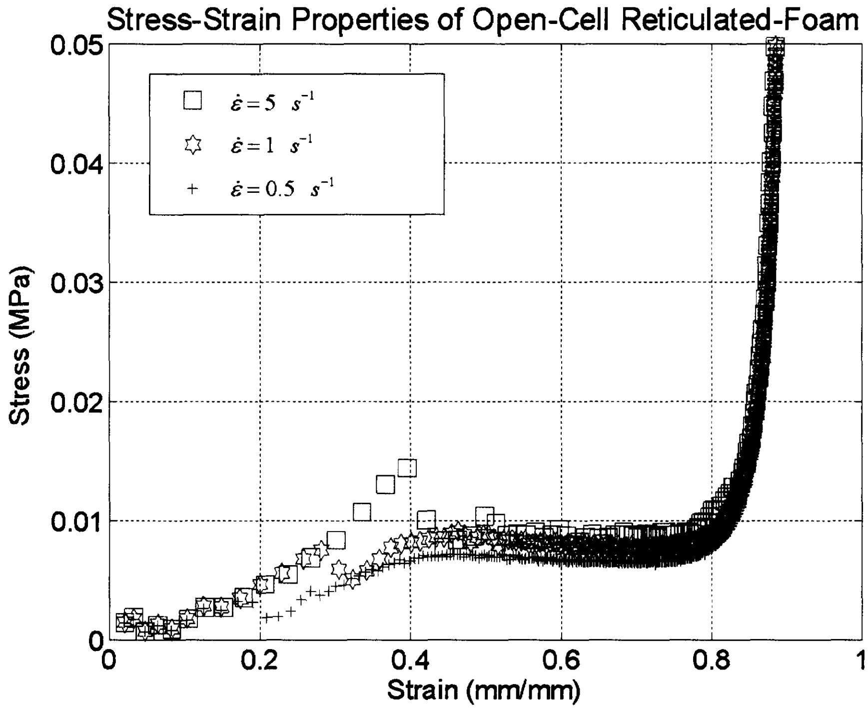

Figure 13: **Stress-Strain Results for constant strain-rate compression testing of open-cell reticulated polyurethane foam of cell size d=363 μm**

In addition, an energy-absorption diagram, described in section 3.2.3, was calculated for the foam, shown in figure 14.

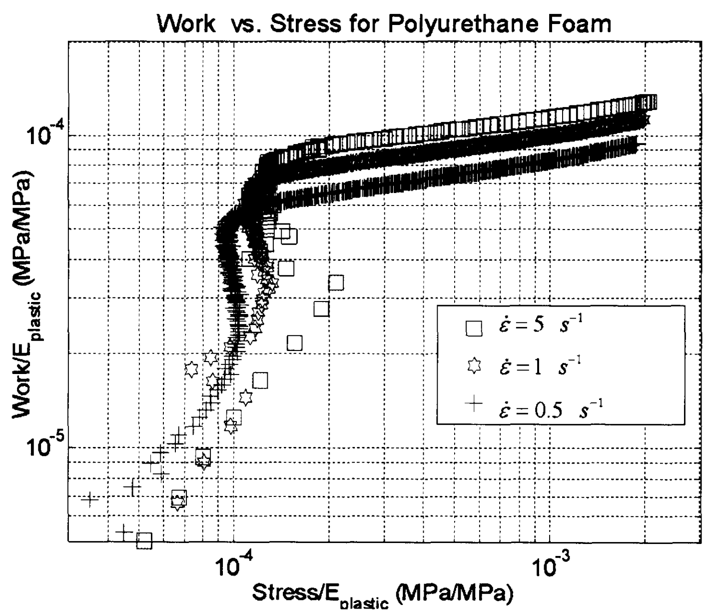

Figure 14 Energy-Absorption Diagram for the open-cell reticulated-polyurethane foam used in this research, of cell size 363 μm

As predicted in figure 9, foams have a compression rate dependence that determines the energy capabilities of the foam. At higher rates, more energy is required to compress the foam at lower strains, due to the increased work of compressing the fluids, air, inside the cell chambers.

6.2.2 Foams Impregnated with Newtonian Fluids

As described in section 5.3.3, the foams were impregnated with glycerol in order to determine the effect of a viscous fluid. The following results demonstrate both the effect of adding fluid to the foams as well as the contribution of the volume fraction to the mechanical properties of the foams, see figures 15. The tests were conducted at a strain rate of 2 s^{-1}.

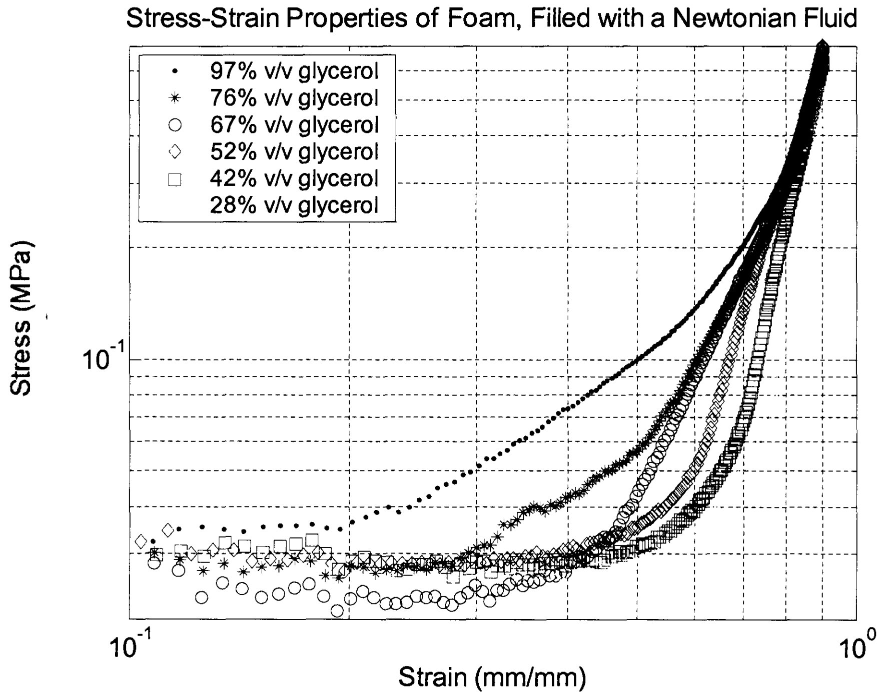

Figure 15 Stress-Strain Results for constant strain-rate compression testing of open-cell reticulated polyurethane foam impregnated with glycerol at various volume fractions (ϕ_v), cell size of 363 μm

6.2.3 Shear-Thickening Fluid Impregnated Foam

Finally, the foams were impregnated with the shear-thickening fluid. The following results demonstrate the impact of the shear-thickening fluids inside the foams, see figures 16. The tests were conducted at a strain rate of 2 s^{-1}.

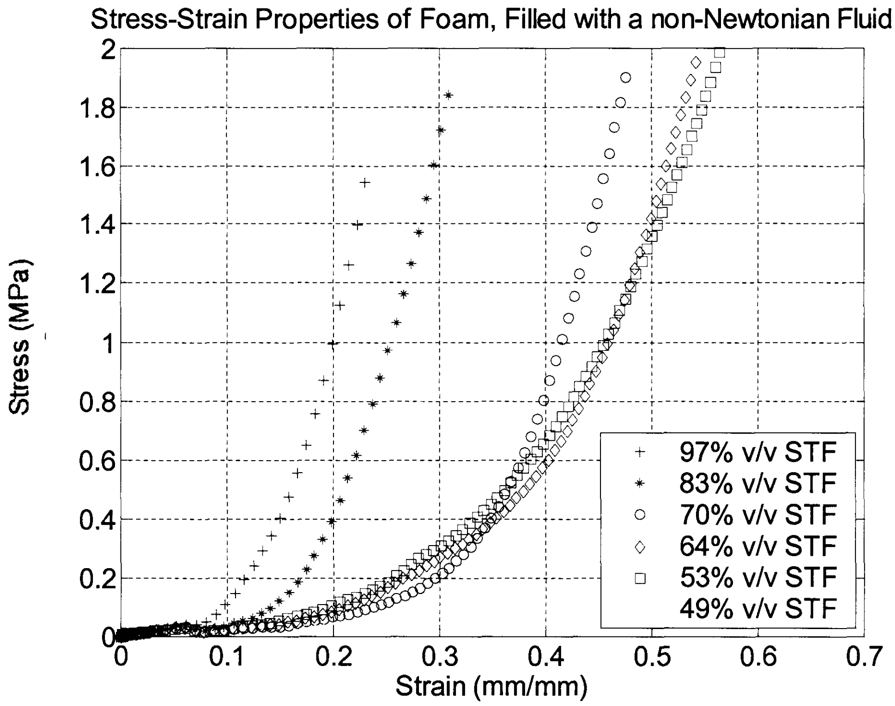

Figure 16 Stress-Strain Results for constant strain-rate compression testing of open-cell reticulated polyurethane foam impregnated with STF at various volume fractions (ϕ_v), cell size of 363 μm

6.2.4 Volume Fraction Dependence of the Shear-Thickening Fluid Filled Foams

In order to determine the accuracy of equation 3.10, it was necessary to vary the volume fraction of STF inside the foams while maintaining all of the other known variables constant. As can be seen by figure 16, the dependence of volume fraction on the mechanical properties is very evident. Several tests were performed with this criterion. In figure 17, the energy absorption diagram was developed for figure 16.

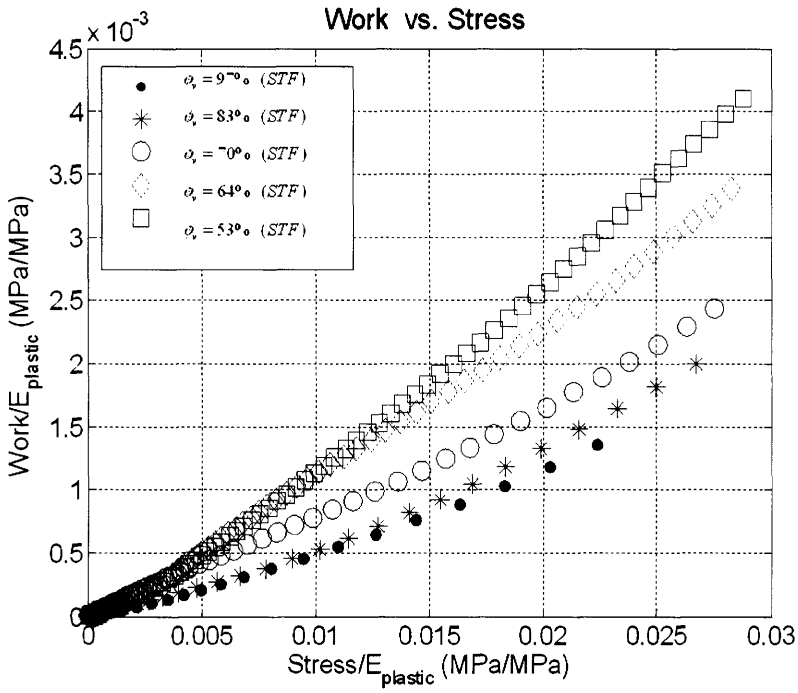

Figure 17 Energy Absorption Diagram for STF filled foam with varying volume fraction, loaded at a constant strain rate $\dot{\varepsilon} = 2\ s^{-1}$

Figures 16 and 17 provided the volume fraction results for values greater than 50%. In these volume fractions, it can be seen that there is a larger amount of work done to compress the foams as the volume fraction decrease. This trend is a result of the foam reaching its densification region at much shorter strains as the volume fraction increases. In addition, volume fraction tests were conducted at lower fractions, ϕ_v<0.53 and the results are presented in figures 18 and 19. In order to delay the onset of shear thickening in the foams, a lower strain rate, $\dot{\varepsilon} = 0.1\ s^{-1}$ was used, but with all parameters equal except for volume fraction.

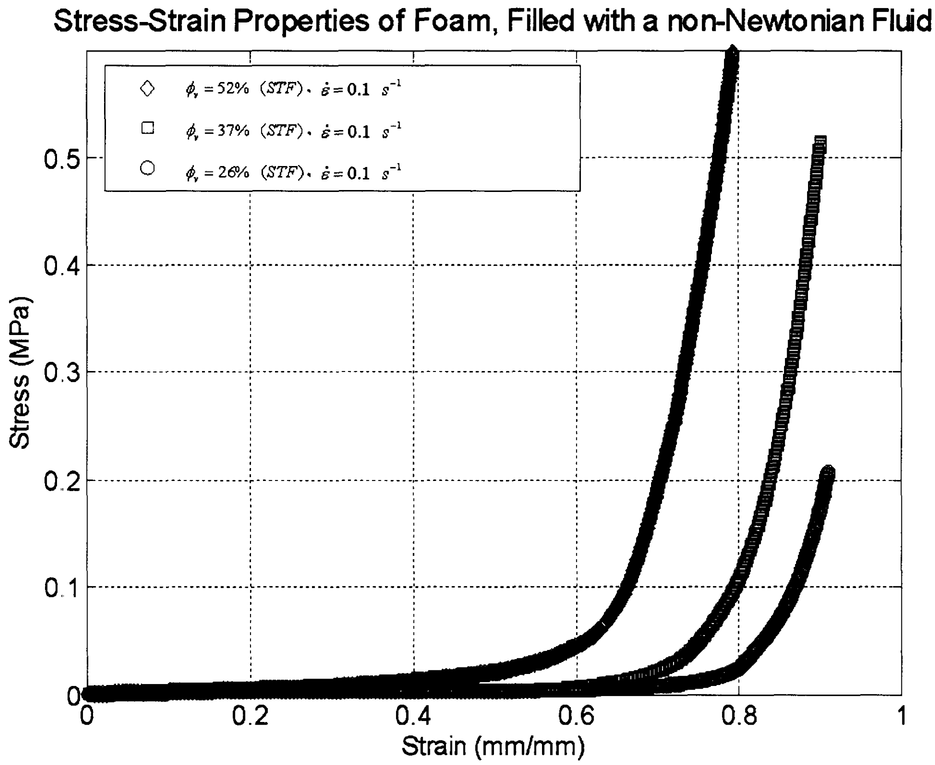

Figure 18 Volume Fraction Dependence of STF filled foams, at volume fractions under 0.53

In these volume fractions, it can be seen that there is a larger amount of work done to compress the foams as the volume fraction increase, opposite to the results shown in figure 17. The increase in work done to compress the foams demonstrates that increasing the volume of fluid in the foam increases the viscous energy dissipation, as depicted in equation 3.6. However, as can be seen from figure 17, an optimal level of volume fraction is necessary during the energy absorption process, in order to avoid early densification.

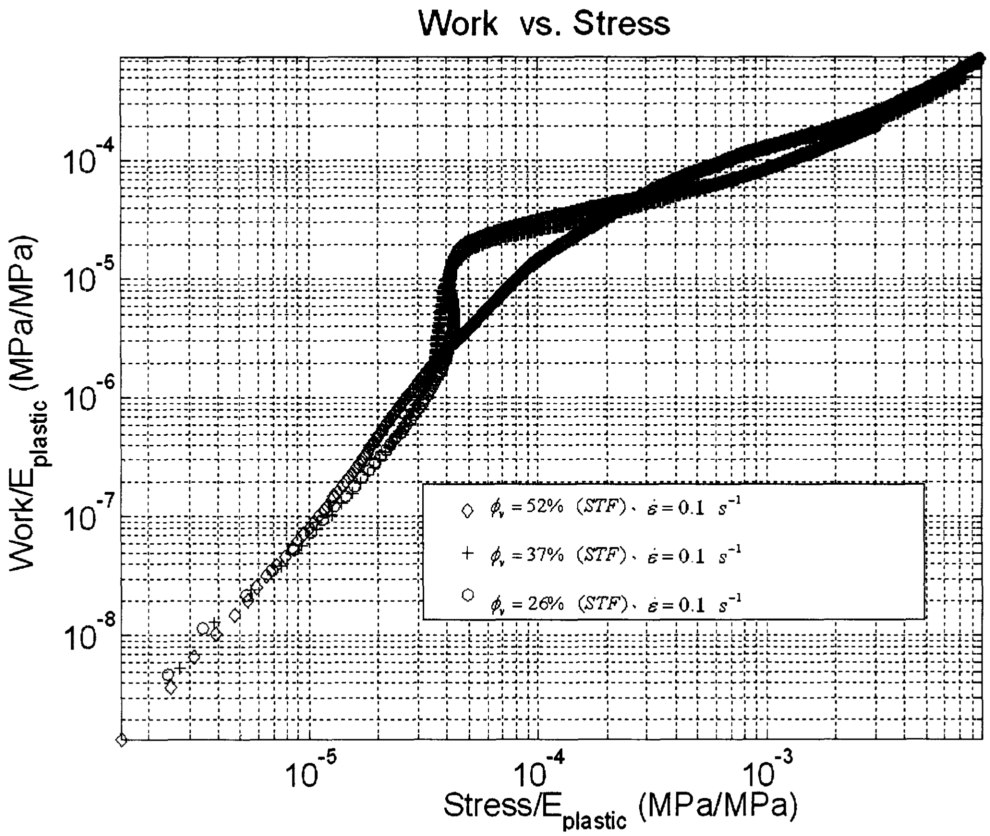

Figure 19 Volume Fraction Dependence of STF filled foams, at volume fractions under 0.53

Similar to Figure 9, as the volume inside the foam increases, the energy absorption capability also increases. However, in dry, empty, foams the increase in energy absorption is related to the relative density of the foam. This correlation is due to the achievement of densification in the foam. However, due to the energy absorption caused by viscous effects within the foam's cell walls, greater work is needed to compress the foam over the same strain. In addition, it can be seen from figure 19 that the typical inflection in the energy diagrams, seen in foams, is attenuated for fluid filled foams at higher volume fractions. This inflection is due to the plateau effect seen in the stress strain diagrams, described by the sequential buckling of the cell walls throughout the foam. Specifically, at the volume fraction of 52%, the inflection is completely attenuated and it is predicted that viscous effects dominate the energy absorption of the system.

6.2.5 Effect of Strain-rate on STF Filled Foams

Equation 3.10 also describes a strong relationship between the external compressive strain-rate placed on the foam to the work done. As such, the loading strain-rate was varied while all of other known variables were kept constant. As can be seen by figure 20, at higher strain rates a larger amount of work was done to compress the foam samples, compared to the low strain rate. This trend is, thus, evidence of the dependence of the loading strain rate on the viscous effect from the fluid flow within the cells. At higher strain-rates, the fluid essentially shear-thickens, increasing the work done by the fluid during the viscous flow out of the cells, as described by equation 3.6.

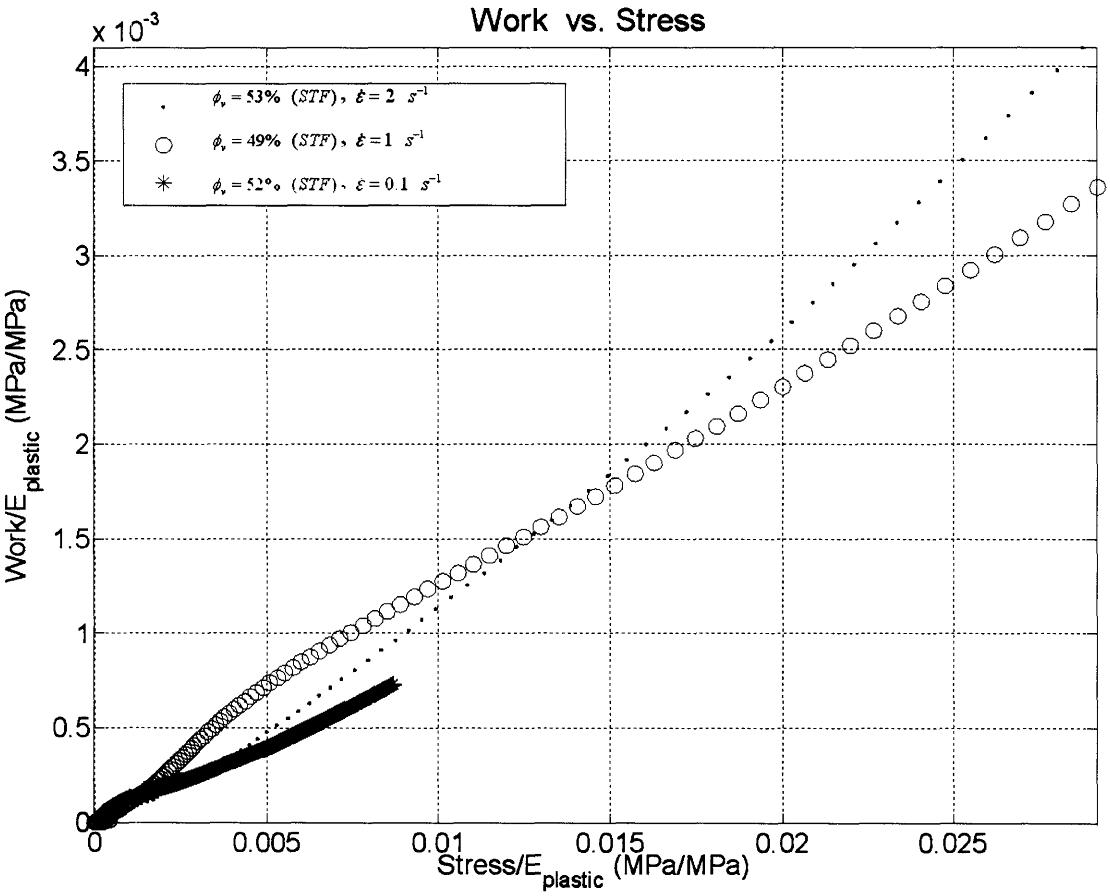

Figure 20 Energy Absorption Diagram for constant volume fraction, ϕ_v ~0.5, but varying compressive strain-rate, $\dot{\varepsilon}$ = 0.1, 1.0, 2.0 s^{-1}

Thus, at higher strain rates, the effect of shear-thickening is more prominent than at lower rates. This effect is a result of the onset of shear-thickening that occurs as a result of the larger hydrodynamic forces induced by the larger strain-rate. This rate dependence demonstrates the shear thickening effect that takes place during the enclosures of the foam cells, as estimated by equation 3.10.

6.2.6 Effect of Newtonian and non-Newtonian Fluids on Foams

In order to characterize the specific effect of STF on the mechanical behavior of foams, a series of comparisons of the mechanical properties of the empty foam, glycerol filled foam, and the STF filled foam are made. In order to justify the effect, the following comparisons were made with all variables kept constant, to include the strain-rate ($\dot{\varepsilon}$), the volume fraction (ϕ_v), and the specific foam used ($\frac{\rho^*}{\rho_s}$). The first comparison takes into consideration the effects when the volume fraction is kept at ϕ_v~0.5, and at a strain rate of $\dot{\varepsilon}$=2 s^{-1}, figures 21 and 22. It can be noted from figure 22 that, although the Newtonian filled foam initially follows the same energy absorption path of the STF filled foam, the STF filled foam surpasses it by almost a factor of three. This energy absorption characteristic is thought to be a product of the shear thickening effect of the STF filled foams. The combination of the volume fraction of STF in the foam, the high strains, which cause the cells to collapse, and the compression strain rates initiate the shear thickening effect in the foams, causing early densification and an increase in energy absorption.

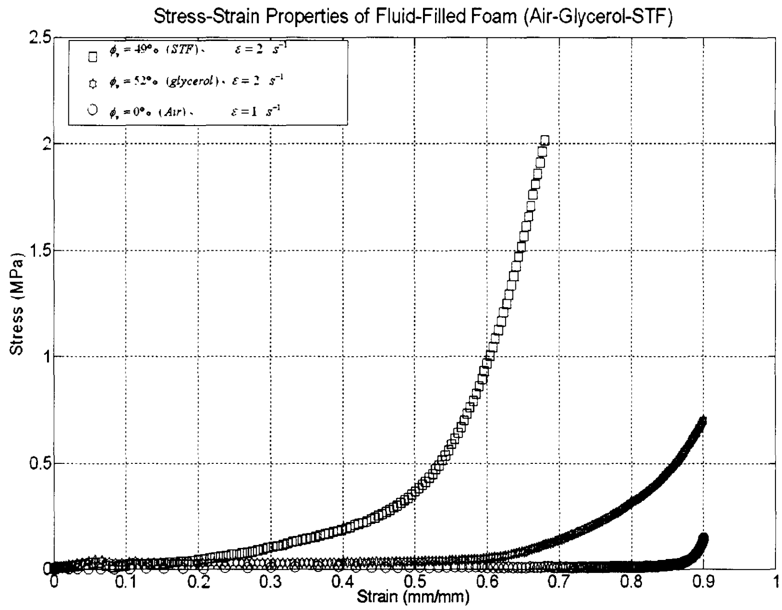

Figure 21 Stress-Strain Properties for foams, at constant volume fraction, ϕ_v ~0.5, and constant compressive strain-rate, $\dot{\varepsilon}$ = 2.0 s^{-1}

As demonstrated in figure 22, the initial viscous energy absorbing effect within the foams is similar for the glycerol and the STF. However, as noted previously, the initiation of shear thickening is the cause for the increase in energy absorption for the same strains.

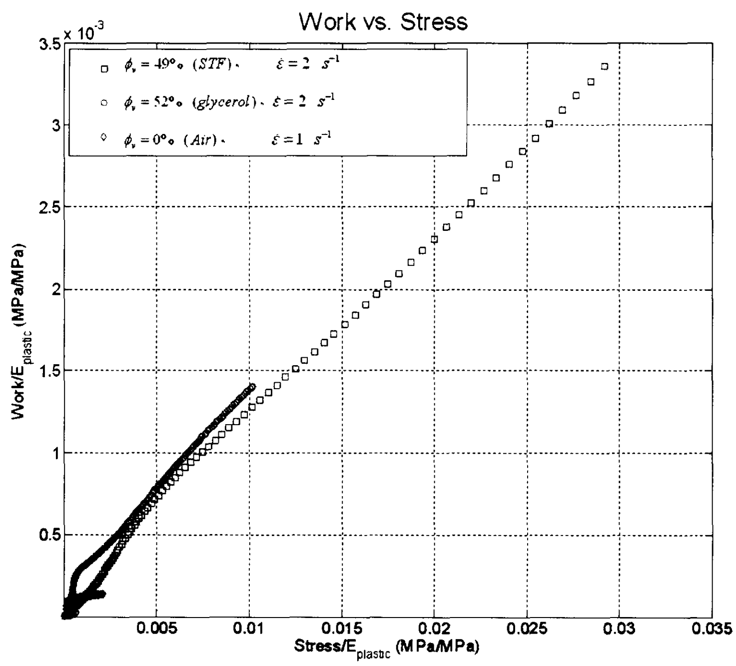

Figure 22 a) Energy Diagram comparing the energy dissipation properties of fluid filled foams.

The Volume Fraction, ϕ_v~0.5, as well as the compressive strain-rate, $\dot{\varepsilon}$ = 2.0 s^{-1}, were kept as constants in these tests.

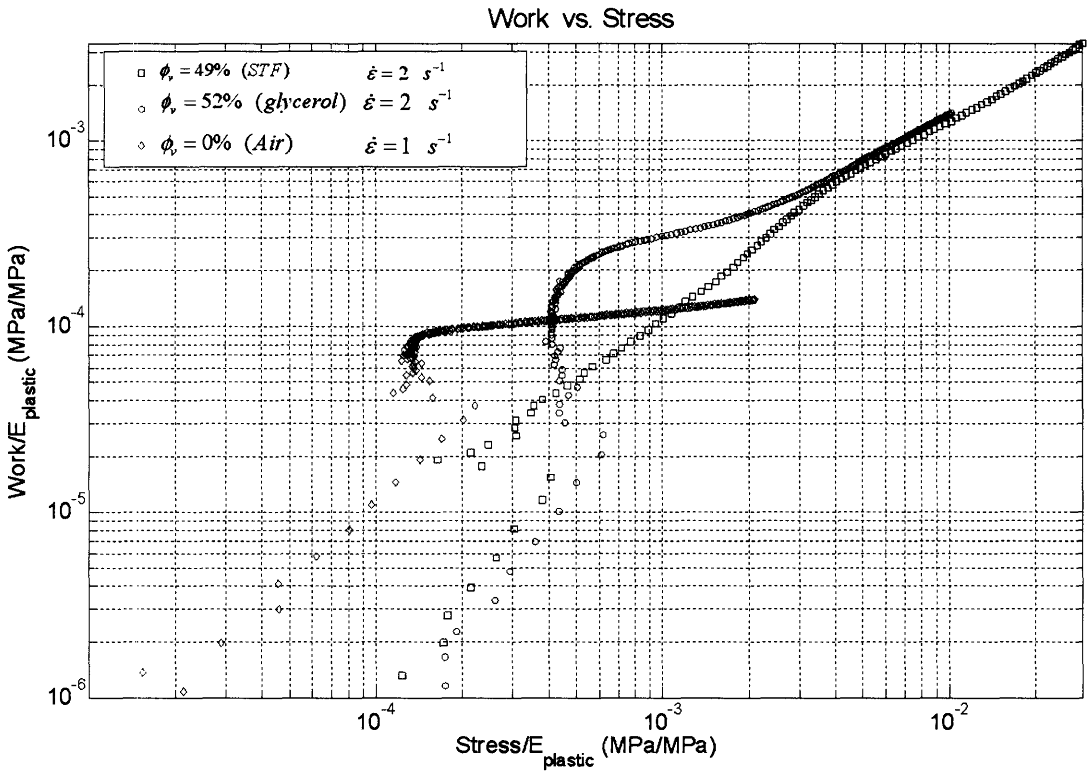

Figure 22 b) Energy Diagram, in a log-log scale, comparing the energy dissipation properties of fluid filled foams. The Volume Fraction, ϕ_v~0.5, as well as the compressive strain-rate, $\dot{\varepsilon}$ = 2.0 s^{-1}, were kept as constants in these tests.

In addition to the previous volume fraction, two other volume fractions, ϕ_v~0.2, 0.9, are explored. As noted before, at low volume fractions, ϕ_v~0.2, the work done by the STF resembles that of the Newtonian fluid in both the stress-strain loading process as well as the energy absorption capabilities.

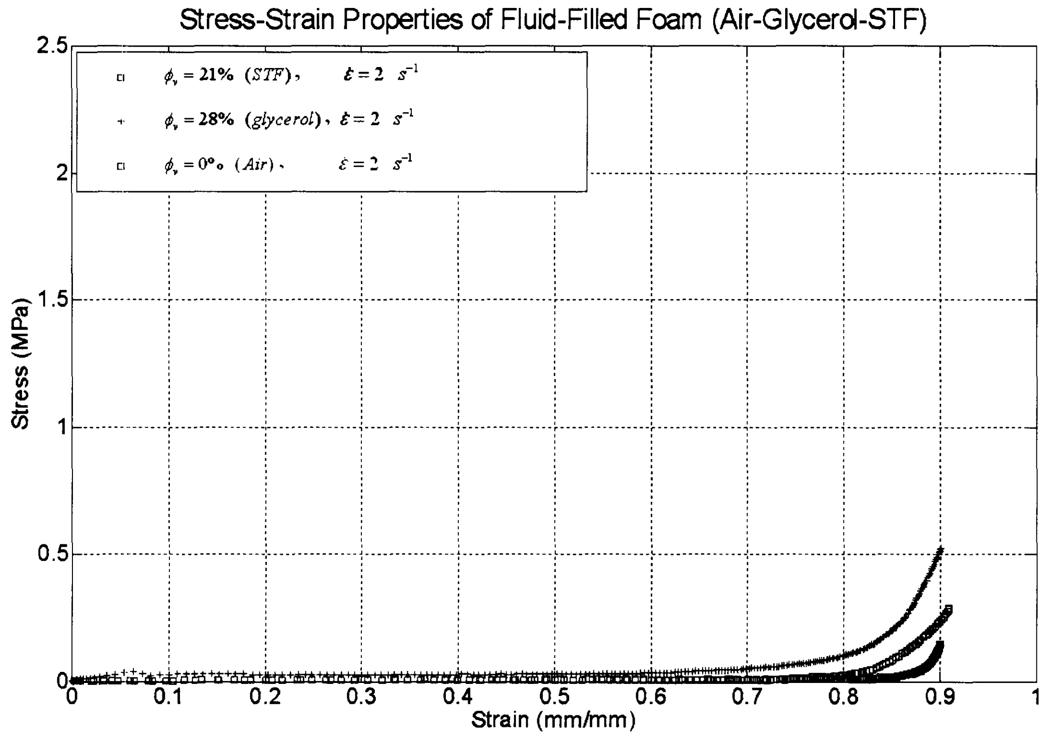

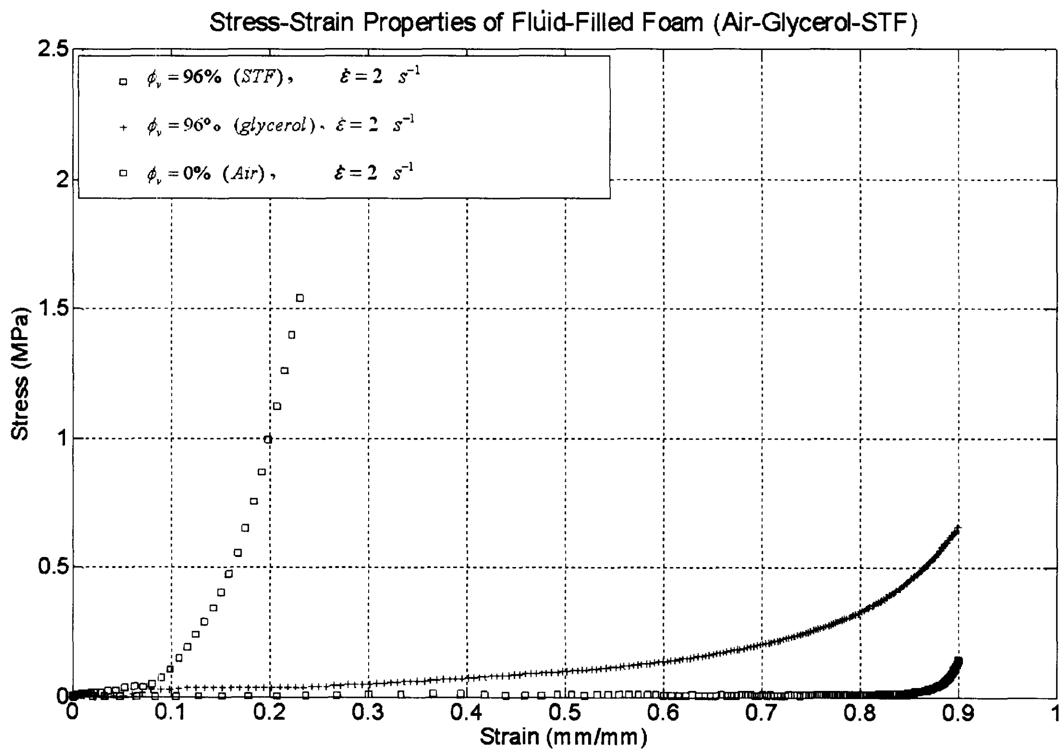

Figure 23 and 24 Stress-Strain Properties for foams, at constant volume fraction, ϕ_v~0.2 and 0.9, and constant compressive strain-rate, $\dot{\varepsilon} = 2.0\ s^{-1}$

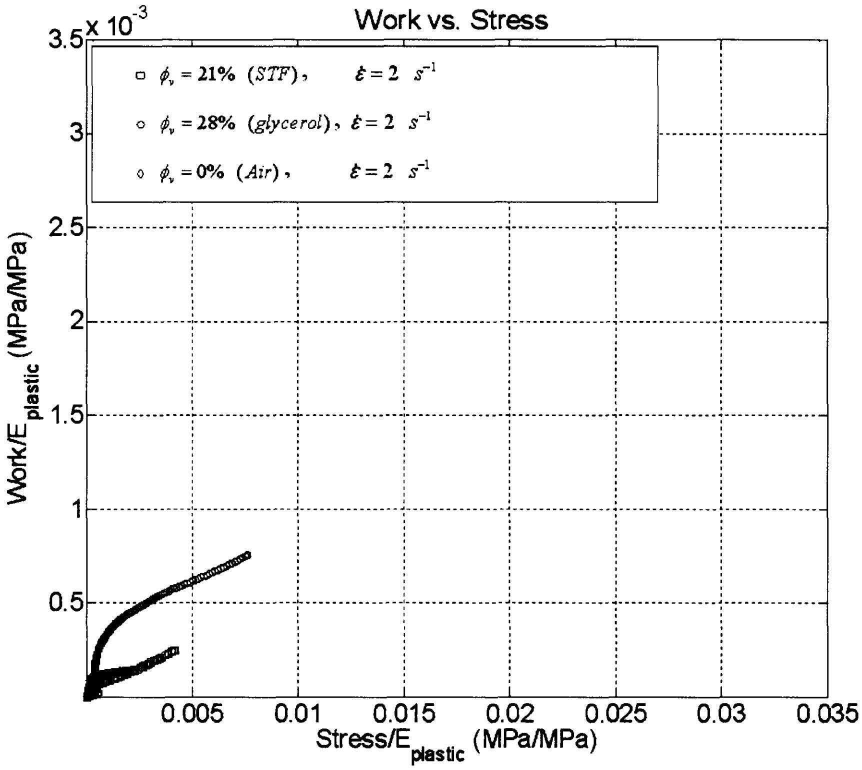

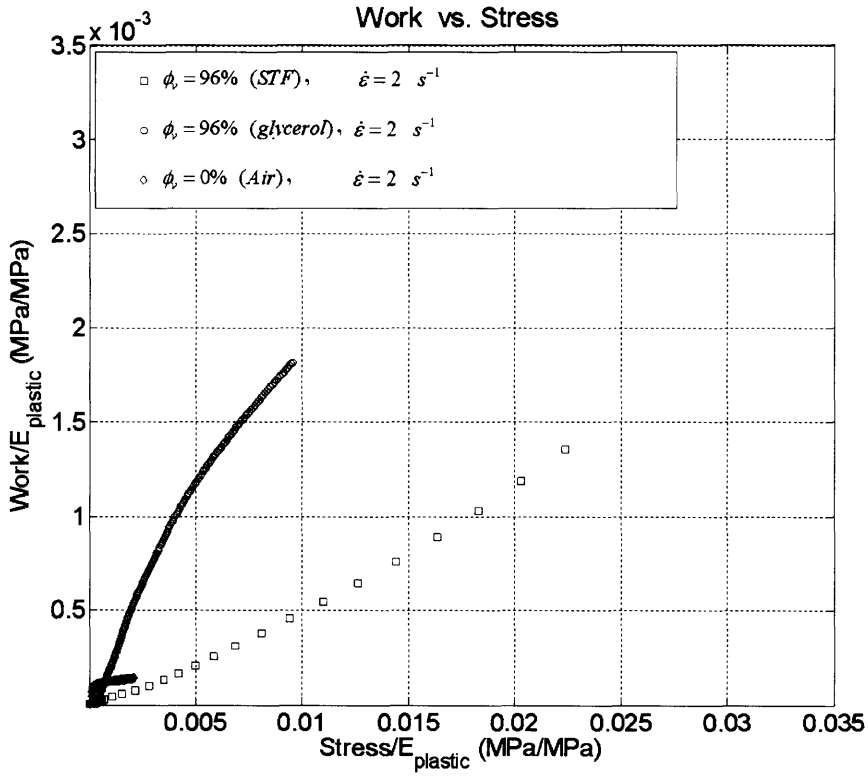

Figure 25 and 26 Energy Absorption Diagram for foams, at constant volume fraction, ϕ_v ~0.2 and 0.9, and constant compressive strain-rate, $\dot{\varepsilon}$ = 2.0 s^{-1}

At high volume fractions, ϕ_v~0.9, the work done by the STF filled foam is not very significant, in comparison with the Newtonian filled-foam, due to the sudden 'rigidity' exhibited by the foam causing it to reach its densification strain quickly.

6.2.7 Summary

The ability of shear-thickening-fluid (STF) filled foams to absorb large amounts of energy has been demonstrated in figures 16 through 26. As predicted by equation 3.6, the model describing the work done by fluid filled foams, the viscosity of the fluid has a large influence on the energy absorption response during compression. In order to validate this observation, a constant viscosity fluid, glycerol, was tested with the same parameters as a non-Newtonian shear-thickening fluid. It was found that at volume fractions above 50%, the influence of shear thickening allowed the STF filled foams to absorb up to twice as much energy as the corresponding Newtonian-fluid filled-foam. Thus, it was found that the volume fraction of the foams had a considerable influence on the energy absorption capabilities of the foams, but with limitations caused by the densification strain. It was also found that the compression strain-rate had a significant impact. Since the strain-rate relates to the critical shear-thickening of the STF, it was found that the activation of this factor contributed to an order of magnitude increase in energy absorption.

7: Conclusions and Future Work

The results of this research were able to provide an initial insight into the analysis of shear-thickening fluid filled foams. The parameters studied were able to correlate the important parameters in this system to the energy absorbing effects that are sought. However, this research is limited in the analysis of several other factors that may also have a large effect. These factors include the relative density of the foams, the contribution of particles size, specific rate dependencies, and the effect of different solvent viscosities used in the shear-thickening fluids. In addition, in order to correlate the various parameters affecting this system, it would be beneficial to have a scaling model that allowed for all variables to be compared in order to have a greater engineering design impact.

9: Bibliography

Barnes, H.A. ''Shear-thickening (Dilatancy) in Suspensions of Nonaggregating Solid Particles Dispersed in Newtonian Liquids.'' *Journal of Rheology* **33**(2): 329–366 (1989).

Bender, J. and Wagner, N. ''Optical measurements of the contributions of colloidal forces to the Rheology of concentrated suspensions,'' *Journal of Colloid and Interface Science*. **172**: 171–184 (1995).

Boersma, W.H., Laven J., and Stein, H.N. ''Shear thickening (Dilatancy) in concentrated suspensions,'' *AIChE Journal*. **36**(3): 321–332 (1990).

Boersma, W.H., Baets, P.J., Laven J., and Stein, H.N. ''Time-dependent behavior and wall slip in concentrated shear thickening suspensions,'' *Journal of Rheology* **35**(6): 1093–1120 (1991).

Deshmukh, S.S. ''Field-Responsive ('Smart') Fluids for Advanced Automotive Applications.'' M.S.. Thesis, Massachusetts Institute of Technology, Cambridge, MA, 2003.

Hayes, W. C. "Bone Fracture Prevention Garment and Method." **US 599290** (1997).

Hoffman, R.L. ''Explanations for the casue of shear thickening in concentrated colloidal suspensions.'' *Journal of Rheology* **42**(1): 111–123 (1998).

Lee, T. and Lakes, R.S. ''Anisotropic polyurethane foam with Poisson's ratio greater than 1.'' *Journal of Material Science* **32**: 2397–2401 (1997).

Lee, T. and Lakes, R.S. ''Anisotropic polyurethane foam with Poisson's ratio greater than 1.'' *Journal of Material Science* **32**: 2397–2401 (1997).

Lu, G. and Xiao, Z.M. ''Mechanical Properties of Porous Materials.'' *Journal of Porous Materials* **6**: 359-368 (1999).

Perez-Rodriguez, J.L. and Carrera, F. ''Sonication as a tool for preparing nanometric vermiculite particles.'' *Nanotechnology* **13**: 382-387 (2002).

van der Werff, J. C. and de Kruif, C. G. ''Hard-sphere colloidal dispersions: Viscosity as a function of shear rate and volume fraction.'' *Journal of Chemical Physics* **83**: 4717–4725 (1985).